DNA recognition and induced genome modification by a hydroxymethyl-γ tail-clamp peptide nucleic acid

Stanley N. Oyaghire[1,8], **Elias Quijano**[2,3,8], **J. Dinithi R. Perera**[1], **Hanna K. Mandl**[3], **W. Mark Saltzman**[3,4,5,6], **Raman Bahal**[7], **Peter M. Glazer**[1,2,9,*]

[1]Department of Therapeutic Radiology, Yale University School of Medicine, New Haven, CT 06520, USA

[2]Department of Genetics, Yale University School of Medicine, New Haven, CT 06520, USA

[3]Department of Biomedical Engineering, Yale University, New Haven, CT 06511, USA

[4]Department of Chemical & Environmental Engineering, Yale University, New Haven, CT 06511, USA

[5]Department of Cellular & Molecular Physiology, Yale University School of Medicine, New Haven, CT 06520, USA

[6]Department of Dermatology, Yale University School of Medicine, New Haven, CT 06520, USA

[7]Department of Pharmaceutical Sciences, University of Connecticut, Storrs, CT 06269, USA

[8]These authors contributed equally

[9]Lead contact

SUMMARY

Peptide nucleic acids (PNAs) can target and stimulate recombination reactions in genomic DNA. We have reported that γPNA oligomers possessing the diethylene glycol γ-substituent show improved efficacy over unmodified PNAs in stimulating recombination-induced gene modification. However, this structural modification poses a challenge because of the inherent racemization risk in *O*-alkylation of the precursory serine side chain. To circumvent this risk and improve γPNA accessibility, we explore the utility of γPNA oligomers possessing the hydroxymethyl-γ moiety for gene-editing applications. We demonstrate that a γPNA oligomer possessing the hydroxymethyl modification, despite weaker preorganization, retains the ability to form a hybrid with the double-stranded DNA target of comparable stability and with higher affinity than that of the diethylene glycol-γPNA. When formulated into poly(lactic-co-glycolic

acid) nanoparticles, the hydroxymethyl-γPNA stimulates higher frequencies (1.5-fold) of gene modification than the diethylene glycol γPNA in mouse bone marrow cells.

Graphical Abstract
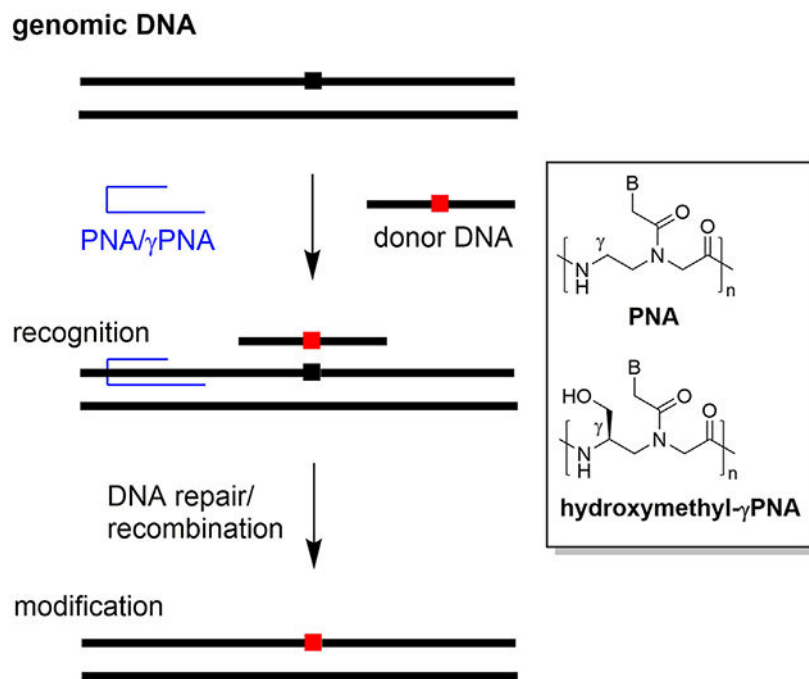
Oyaghire et al. show that hydroxymethyl-γ-modified PNAs retain the helical pre-organization present in the more elaborate diethylene glycol-γ-modified PNAs but are more efficient at strand invasion and gene modification. This finding obviates the need for elaborate synthetic steps needed to obtain custom PNA oligomers useful for biochemical studies related to DNA recognition.

INTRODUCTION

Peptide nucleic acids (PNAs) that bind to and stimulate recombination events in genomic DNA are useful reagents for genome editing[1-8] and avoid or minimize the emerging limitations of nuclease-based[9-11] reagents (like CRISPR-Cas9) such as genotoxicity[12-16] and immunogenicity.[17,18] Developed as nucleic acid mimics and ligands,[19,20] PNA oligomers bind DNA targets with high affinity, activating—in the context of genomic DNA— endogenous DNA repair pathways that mediate incorporation of co-supplied donor DNA oligomers carrying the intended sequence changes at the target (homologous) site.[1] Further, PNAs' binding specificity[21] restricts repair activation and resultant gene modification to genomic regions at/proximal to the PNA binding site,[22-24] allowing for gene editing to proceed with low off-target effects.[5-8] Importantly, when encapsulated in and delivered by poly(lactic-co-glycolic acid) (PLGA) nanoparticles (NPs),[25] PNA/donor oligomers mediate gene correction at frequencies sufficient to reverse disease phenotypes in mice.[6-8]

The efficacy of PNA oligomers for gene editing is connected to their affinity for complementary DNA targets that can exist transiently as accessible single strands during

DNA replication and gene transcription, for example, but predominantly as compact duplex structures.[26] For example, we demonstrated that the editing efficacy of a bisPNA oligomer[27]—which contains domains to recognize the Watson-Crick and Hoogsteen faces of a DNA target—was enhanced 5-fold by extending the binding domain on the Watson-Crick face, as in a tail-clamp (tc) PNA design,[28] due to improved DNA invasion/binding.[5] Also, we recently reported that the incorporation of γPNA[29,30] monomers—derivatives that improve affinity and specificity of composite oligomers[29] and their ability to invade B-DNA[31]—in a tcPNA oligomer increased editing frequency 2-fold over the unmodified tcPNA.[5] The γPNA modification has been shown to drive conformational selection in PNA oligomers by inducing a network of steric clashes and nucleobase stacking interactions,[30] with the resultant helical sense determined by the stereochemistry at the PNA γ-position.[32] Specifically, the R configuration in γPNA monomers induces PNA oligomers to adopt a right-handed helical conformation as single, unbound strands[30]—the same orientation enforced on them upon binding to complementary DNA/RNA targets.[33] This preorganization reduces the entropic cost of DNA binding, an effect that accelerates hybridization to single-stranded (ss) targets[29] and enhances strand invasion of duplex targets.[31]

The chemical moiety at the γ-position primarily depends on the nature of the precursory amino acid side chain,[30,34-40] although additional synthetic derivatization is possible.[29,41-43] To date, however, only γPNA monomers possessing the diethylene glycol (also called minipeg [mp][29]) γ-substituent have been tested for gene-editing applications and have been shown to enhance editing frequencies over unmodified PNAs.[7,8] mp-modified γPNAs ([mp]γPNAs) retain all the biophysical features and improved binding properties of γPNA oligomers outlined above and possess enhanced aqueous solubility due to the hydrophilic mp moiety.[29] However, synthesis of the requisite monomers is challenging, primarily because of the racemization risk inherent in the crucial O-alkylation step to incorporate the mp unit onto the serine side chain.[29] In this regard, various safeguards have been utilized to obtain optically pure monomers—ranging from careful control[29] of reaction temperature and time and reagent addition order to *in situ*[29] or precursory[44] derivatization of serine to minimize the acidity of the alpha proton. However, these precautions do not obviate the need for further analytical validation of optical purity,[29,44] a parameter especially salient in gene editing, since monomers with even minute (5%) racemates significantly compromise DNA affinity.[45]

We examined here whether γPNA oligomers possessing the hydroxymethyl-γ-substituent would be effective reagents for gene editing. As this moiety is directly accessible from the serine side chain (hence [ser]γPNA), monomer synthesis circumvents the stereochemical contamination risk inherent in O-alkylation, simplifying the synthetic procedure considerably, as has been reported.[30,39,40] We synthesized a [ser]γPNA (from commercially available monomers) and compared its helical organization, DNA-binding properties, and gene-editing frequencies to a known isosequential [mp]γPNA.[7] Although possessing the less elaborate γ-substituent, [ser]γPNA preserves (but relaxes) the helical organization inherent in [mp]γPNA. Surprisingly, the thermodynamic stabilities of hybrids formed with a double-stranded DNA target are comparable for both [ser]γPNA and [mp]γPNA, in both low- and high-salt buffers, even with the weaker preorganization in the former.

Importantly, we show that $^{ser}\gamma$PNA induces higher (1.5-fold) editing frequencies with two different donor DNA oligomers, relative to $^{mp}\gamma$PNA, in bone marrow cells from two different transgenic animals.

RESULTS

Rationale and γPNA design

We previously reported that a tcPNA oligomer (PNA; Scheme 1) designed to bind 70 bp upstream of the position of a β-thalassemia-associated mutation was able to stimulate recombination of a donor DNA oligomer with the target homologous region in genomic DNA.[7] The tcPNA design has binding domains that recognize the Watson-Crick and Hoogsteen faces of a purine-rich sequence of the DNA target, with an extended recognition sequence on the Watson-Crick domain.[28] Modification of PNA with γPNA residues bearing the diethylene glycol γ-substituent on the Watson-Crick domain ($^{mp}\gamma$PNA; Scheme 1) improved editing frequencies 2- to 3-fold *ex vivo* due to enhanced DNA binding. NP-mediated administration of this PNA reversed thalassemic phenotypes in mouse models *in vivo*.[7,8] To obviate the need for the elaborate chemical syntheses required to install the diethylene glycol unit in the precursor serine side chain,[29,44] we explored whether a tcPNA bearing just hydroxymethyl-γ-substituents, themselves directly derivable from serine ($^{ser}\gamma$PNA; Scheme 1), would retain the biophysical and DNA hybridization properties of $^{mp}\gamma$PNA and remain superior for gene editing relative to PNA.

Helical organization of PNA and γPNAs

We first sought to examine the effects of $^{mp}\gamma$- or $^{ser}\gamma$-PNA residues (Scheme 1, Table 1) on the global helical structure of the composite tcPNA oligomers using circular dichroism (CD) experiments, which have previously been utilized for characterization of γPNA helical conformation.[29,30,46] Our experiments show that samples containing equimolar amounts of the $^{ser}\gamma$PNA or $^{mp}\gamma$PNA oligomers display local minimum and maximum at 240 and 267 nm, respectively (in addition to the other peaks), both of which are absent in the unmodified PNA oligomer (Figure 1). The position (λ) and orientation (minima/maxima) of this specific exciton coupling pattern are consistent with the adoption of a right-handed helical structure.[47] However, the more pronounced 240 nm minimum observed for $^{mp}\gamma$PNA suggests that it is more helically preorganized[29] than $^{ser}\gamma$PNA. It is likely that the steric clashes in the γPNA back-bone, which potentiate conformational selection in the oligomer, will be greater with the larger diethylene glycol ($^{mp}\gamma$PNA) than with hydroxymethyl ($^{ser}\gamma$PNA) as the γ-substituent, as suggested[48] and demonstrated[32] by Ly and co-workers.

While helical organization occurs to varying degrees, it is concentration independent for both, as demonstrated by the linear correlation between signal amplitude and oligomer concentration (Figure S1), suggesting that the observed effects are intrinsic to the molecules themselves, as previously observed,[30] and are uninfluenced by aggregation or intermolecular complexation in solution. Interestingly, regardless of the absence or degree of helical organization in the PNA/γPNA oligomers, their hybrid triplexes with a complementary ssDNA target have similar helical structures (Figure 2), indicating that γ modifications of either kind do not affect the conformation of the thermodynamic product from the binding

reaction. The same trend was observed for PNA/γPNA binding in the context of a dsDNA target (Figure S2).

Thermal stability of PNA/γPNA-DNA hybrids

We next sought to characterize the thermal stabilities of the hybrid complexes by recording ultraviolet (UV) absorbance at 265 nm with increasing temperature. Initial analyses on hybrids formed with the 100-nt ssDNA target with overhangs (Figure S3A) and an ssDNA target without overhangs (Figure S3B) both yielded incomplete melting transitions. The non-cooperative melting observed with the 100-nt ssDNA is likely due to the "overhang effect," whereby the overhanging bases stack upon the bound duplex, providing further stabilization beyond the Watson-Crick pairs.[49,50] We also present data (Figure 3) for hybrids formed with a double-stranded DNA (dsDNA) target preassembled by annealing ssDNA with the PNA and then with its complement. The dsDNA-PNA/γPNA hybrids were assembled under conditions where complete dsDNA binding was observed by gel shift (Figure 4), enabling unambiguous attribution of the melting transitions to dissociation of the hybrid complex rather than to contributions from partially PNA-bound and free dsDNA.

We observe that the hybrid complexes are less thermally stable than the free dsDNA (− T = 15°C–17°C; Figure 3A; Table 2) in 10 mM NaPi, consistent with a binding model where PNA/γPNA hybridization to the target strand is accompanied by displacement of the homologous region on the non-target DNA strand. In this model, the hyperchromicity accompanying melting likely reflects the release of the non-target strand from the PNA-bound target strand, since ssDNA-PNA/γPNA hybrids show incomplete transitions. Further, similar analyses at 100 mM NaPi show that although the same binding-induced duplex destabilization occurs, the melting temperatures for the hybrids are higher (Figures 3B; Table 2) than those at 10 mM NaPi, presumably because the DNA-DNA base pairs flanking the PNA-bound region are made more stable at the higher salt concentration (Figure S5).

We also performed van't Hoff analyses of the melting profiles using the protocols outlined by Marky and Breslauer.[51] As outlined in Figure S3, no cooperative melting transitions are observed with the ssDNA-PNA/γPNA duplexes. Therefore, the melting transitions observed in Figure 3 are attributable to DNA-DNA duplexes flanking the DNA-PNA/γPNA complex, as illustrated in Figure S5. We observe DNA duplex formation as an exergonic process in the presence of all PNA/γPNAs at 10 and 100 mM NaPi (− G = 34–35 and 41–48 kcal mol^{-1}, respectively [Table 2]). The duplexes are more stable at 100 mM NaPi, an unsurprising trend in our model since the DNA-DNA base pairs on either side of the PNA-DNA hybrid, which remain unperturbed by PNA recognition, would be more stable under this condition. Because PNAs/γPNAs readily hybridize to their ssDNA targets, the free energies observed in either salt condition represent the binding energies associated with annealing of the non-target DNA oligomer to the unhybridized nucleotides in the ssDNA-PNA/γPNA duplex. The data in Table 2 suggest that the free energy change for this DNA-DNA hybridization reaction is unaffected by the nature of PNA bound to the target DNA oligomer at low-salt concentration. However, there is a systematic decrease in the free energy change of this reaction with increasing preorganization on the PNA strand in 100 mM NaPi. It is possible that the increased rigidity introduced to the target DNA oligomer upon ^{mp}γPNA or ^{ser}γPNA

binding stabilizes alternative conformations in the flanking nucleotides, making them less accessible to the complementary bases on the non-target DNA oligomer.

DNA invasion by PNAs/γPNAs

To evaluate the relative binding affinities of the PNAs/γPNAs for strand invasion toward a duplex DNA target, we titrated increasing equivalents of the respective PNAs into 50 nM target dsDNA (100-mer) in 100 mM NaPi buffer. Compared with ^{mp}γPNA and PNA, ^{Ser}γPNA showed superior strand invasion and binding to dsDNA (Figure 4). The concentration of PNA/γPNA-DNA complex formed with increasing PNA/γPNA concentration was fit to a Langmuir isotherm that accounts for ligand depletion. Dose-response plots and binding isotherms for each PNA/γPNA are presented in Figure 5, and the calculated equilibrium dissociation constants are provided in Table 3. We observe that ^{ser}γPNA has ~19- and ~ 11 -fold higher affinity than PNA and ^{mp}γPNA, respectively.

NP formulation and characterization

Previously, we demonstrated that NPs made of PLGA could effectively encapsulate and deliver PNA and donor DNA to correct mutations underlying β-thalassemia *in vivo* in adult[7] and fetal mice.[8] Using a similar approach, we synthesized PLGA NPs encapsulating ^{mp}γPNA or ^{ser}γPNA along with donor DNA to correct or introduce the same IVS2-654 mutation.[7,8] The physiochemical characteristics of these NP formulations did not differ significantly between both γPNAs (Figure 6). Average NP diameters were 270 nm for ^{mp}γPNA and 290 nm for ^{ser}γPNA, as measured by dynamic light scattering (DLS) (Figure 6A) and imaged by transmission electron microscopy (TEM) (Figure S6). The TEM images demonstrate spherical morphology consistent with DLS. Likewise, NP surface charge was similar between both formulations, at −19 mV for ^{mp}γPNA and −24 mV for ^{ser}γPNA NPs (Figure 6B). Similarly, average total nucleic acid loading did not differ significantly (Figure 6C). Despite differences in chemical modification, both PNAs displayed similar release rates, with greater than 50% of total nucleic acid content being released for each formulation after 72 h (Figure 6D).

Correction of the β-thalassemia mutation in primary HSPCs

Given the physiochemical similarities between the NPs, we hypothesized that the superior hybridization and duplex invasion properties of ^{ser}γPNA would result in higher levels of gene editing relative to ^{mp}γPNA. To test this hypothesis, we started by designing a donor DNA to introduce the IVS2-654 mutation. NPs were subsequently formulated to encapsulate this "mutating" donor DNA and ^{mp}γPNA or ^{ser}γPNA. Primary bone marrow cells from mice with a wild-type human β-globin transgene were isolated and treated with 2 mg mL^{-1} PLGA NPs. We found (Figure 7) that NPs encapsulating ^{ser}γPNA achieved significantly higher levels of genome modification, as measured by a droplet digital PCR (ddPCR) assay previously optimized to detect the wild-type and mutant alleles in genomic DNA.[8]

We next sought to determine whether ^{ser}γPNA could induce gene correction in bone marrow from a mouse model of β-thalassemia with the IVS2-654 mutation. As before, NPs were formulated with ^{mp}γPNA or ^{ser}γPNA but this time also with a "correcting" donor DNA. Primary bone marrow cells from these mice were treated with 2 mg mL^{-1} PLGA NPs.

Again, gene correction of the underlying β-thalassemia mutation was significantly higher with ^{ser}γPNA (Figure 8), despite similarities in all the measured physiochemical properties of the NPs themselves. We also compared editing of ^{ser}γPNA with ^{ser}γPNA-scr and confirmed minimal editing with the scrambled oligomer compared to the targeting PNA (Figure S4). Furthermore, to evaluate the cell toxicity of the PNA-NPs, we carried out cell viability analysis using CellTiter-Glo luminescent cell viability assay on NP-treated mouse primary bone marrow cells. The PNA-NPs showed no toxicity in the treated cells when accessed from 24 h to 7 days post-treatment, confirming the safely of the PNA-NPs (Figure S7). Taken together, these experiments show the superiority of ^{ser}γPNA compared with ^{mp}γPNA in inducing genome modification, as observed in two distinct primary cell lines with two distinct donor DNA sequences.

DISCUSSION

We present data on the biophysical and DNA-binding properties of a tcPNA oligomer possessing a hydroxymethyl-γ (^{ser}γ)-substituent and compare/contrast these with measurements with an isosequential oligomer with the mp-γ modification (^{mp}γ). Our results indicate that, as unbound molecules, both oligomers adopt a right-handed helical conformation, as predicted from the configuration of the γ-stereogenic center.[29,30] Helical organization is more pronounced for ^{mp}γPNA than for ^{ser}γPNA, an observation predictable from the relative sizes of the chemical moieties at the γ-position[32] (diethylene glycol and hydroxymethyl, respectively). DNA recognition in the context of a duplex target yields hybrids of comparable stabilities for both ^{ser}γPNA and ^{mp}γPNA, and we observe strand invasion of hydroxymethyl-γPNA to be superior to that of diethylene glycol-γPNA.

Because the ^{mp}γPNA examined in this work was previously reported to mediate genotypic and phenotypic correction in β-thalassemic mice,[7,8] we evaluated the efficacy of ^{ser}γPNA for genome modification in bone marrow cells from transgenic mice harboring the human β-globin gene and possessing a wild-type or mutant genotype at the relevant thalassemia-associated locus. In both formats, ^{ser}γPNA induced higher gene-editing frequencies than ^{mp}γPNA, a trend not attributable to any differences in the physicochemical properties of the PLGA NPs synthesized to encapsulate and deliver the respective γPNA/donor DNA reagents. Taken together, our results show that the hydroxymethyl-γ modification, which is directly accessible via the serine side chain and circumvents the synthetic limitations and racemization risks inherent in elaborate modification at the γ-position[29,44] (as in ^{mp}γ), can be used as an alternative to the more specialized diethylene glycol-γ modification, yielding composite γPNA oligomers that show comparable DNA recognition properties and gene modification frequencies.

While they have been repurposed here, for the first time, as viable alternative/improved co-reagents for mediating PNA-induced gene modification, ^{ser}γ-modified PNAs are not new in the literature of PNA-based nucleic acid ligands. In their seminal work describing the effects of PNA backbone γ substitutions on the global oligomer structure, Ly and co-workers[30] demonstrated that incorporation of hydroxymethyl-γ-residues in a PNA oligomer introduced defined steric clashes in the PNA backbone that initiated a unidirectional helical preorganization.[30] They further showed that complete or partial modification of the PNA

oligomer with this substituent, as with other moieties[29,43,48,52] introduced at the same position, resulted in improved binding to target DNA/RNA and enhanced selectivity against non-target strands compared to classic-PNAs.[30] Romanelli and co-workers subsequently showed that PNA oligomers sparingly modified with [ser]γ-residues effectively perturbed Sp1 recognition of a duplex DNA target modeled after its binding sequence in cognate promoters.[40] Virta and co-workers have also introduced these modifications into a PNA oligomer designed to target a model microRNA hairpin structure.[39] Our work extends these prior studies by demonstrating the superiority of the [ser]γ-modified PNAs for binding to duplex DNA and for gene editing in primary bone marrow cells.

The utility of [ser]γPNA in gene-editing applications raises the question of what other existing[34-38,41,42] or novel γ modifications may be repurposed or developed for similar ends, especially if they are more synthetically and/or commercially accessible than existing reagents. While we consider this question to be an interesting area for future study, we believe that at least two parameters should guide explorations on this theme: (1) hydrophilicity of the γ-substituents to preserve the aqueous solubility of the [mp]γ-modified PNA reagents and (2) substituent size in order to retain the steric clashes that initiate conformational selection in the oligomer. For the latter, careful tuning will be required to ensure that conformational preorganization to improve binding affinity/kinetics does not sacrifice conformational flexibility to accommodate the structural dynamics of the target DNA.

To liberalize reagent access even further, it is worth exploring the minimum number of γ modifications (of any kind) required to improve the editing efficacy relative to the base PNA sequence. Should the [ser]γ and [mp]γ modifications prove superior to others reported, such studies, coupled with the directionality[30] of helical induction, might significantly reduce PNA reagent costs by directing users toward fewer modifications. However, while much of this work should continue, we believe that therapeutic utility of this editing modality will be made more likely by a combination of optimization efforts on all three components (polymer/PNA/donor DNA) of the NP reagents.

EXPERIMENTAL PROCEDURES

Resource availability

Lead contact—Further requests for information should be directed to and will be fulfilled by the lead contact, Peter M. Glazer (peter.glazer@yale.edu).

Materials availability—This study did not generate new unique materials.

Data and code availability—This study did not generate/analyze datasets/code.

PNAs and DNAs

The sequences for all PNA and γPNA oligomers used in this study targeting the human β-globin gene were previously published[7] and are presented in Table 1 with the addition of a sequence containing hydroxymethyl-γ-modified bases ([ser]γPNA). All hydroxymethyl-γPNA monomers were purchased from ASM Research Chemicals (Hannover, Germany)

and featured tert-butyloxycarbonyl (boc) and benzyl (Bn) moieties as the protecting groups on the backbone amino and side-chain hydroxyl groups, respectively. The unmodified tcPNA oligomer (designated henceforth as PNA) and the mp-γ-modified tcPNA (^mpγPNA) were obtained from TruCode Gene Repair (San Francisco, CA, USA). We also included ^serγPNA-scr (Table 1) as a scrambled sequence control. DNA oligomers utilized for binding and/or melting experiments were purchased from Integrated DNA Technologies (https://idtdna.com) as either unmodified or 5′-biotinylated derivatives, and their sequences are presented in the relevant experimental procedures sections. 50:50 Poly(DL-lactide-co-glycolide), an ester terminated with an inherent viscosity 0.55–0.75 (dL/g), was purchased from LACTEL Absorbable Polymers (Birmingham, AL, USA). Poly(vinyl alcohol) (PVA), average molecular weight 30,000–70,000, was purchased from Sigma-Aldrich (St. Louis, MO, USA). Dichloromethane was purchased from Sigma-Aldrich. To test for gene editing by ^mpγPNA and ^serγPNA, we designed 60-nt ss donor DNAs to either introduce the IVS2-654 mutation or to correct it. The sequences for donor DNAs are provided below, with the intended sequence change highlighted in bold. All DNA donors contain three phosphorothioate internucleoside linkages at each end to protect from nuclease degradation.

Correcting donor (5′-3′):
AAAGAATAACAGTGATAATTTCTGGGTTAAGG**C**AATAGCAATATCTCTGCATATAA ATAT.

Mutating donor (5′-3′):
AAAGAATAACAGTGATAATTTCTGGGTTAAGG**T**AATAGCAATATCTCTGCATATAAA TAT.

PNA synthesis, purification, and characterization

Oligomer synthesis was performed using previously established protocols for standard solid-phase PNA synthesis.[53] Synthesis began on an MBHA solid support (resin) labeled in-house with a lysine residue. The entire synthesis consisted of iterative cycles of two major steps: (1) amine deprotection with a solution of trifluoroacetic acid (TFA)/m-cresol (95/5) and (2) monomer coupling with a cocktail of boc/Bn-protected monomers (A, G, T, C, or J), DIEA, and HBTU (1/1.3/0.9) dissolved in N-methyl-2-pyrrolidinone and dimethylformamide (1:1). After completion of the cycle for the last monomer, the oligomer was cleaved (released) by submerging the resin in a solution of m-cresol/thioanisole/TFA/trifluroromethane sulfonic acid (1:1:2:6). The pure product was isolated by reverse-phase (RP) high-performance liquid chromatography (HPLC), using a solvent gradient of acetonitrile and water, and analyzed using MALDI-TOF mass spectrometry.

CD spectropolarimetry

Samples containing increasing concentrations (1–20 μM) of PNA or γPNA oligomers were prepared in a buffer containing 10 mM Na_3PO_4 (NaPi, pH 7.4). For the hybrid complexes, samples containing 1 μM complementary ssDNA and 2 μM PNA/γPNA, or 2.5 μM dsDNA and 5 μM PNA/γPNA, were annealed in the same NaPi buffer. For either sample set, a "blank" sample containing the buffer alone was used as a negative control. The annealing step involved high-temperature (95°C) heating followed by slow cooling to

ambient temperature on a heat block to allow formation of the most stable conformations or secondary structures within/by each PNA/γPNA oligomer or by the respective hybrid complexes. CD spectra were recorded on a Chirascan CD spectropolarimeter (Applied Photophysics). All spectra were collected from 200 to 350 nm, baseline corrected, and recorded as the average of three consecutive scans. The sequences for the DNA oligos used as ssDNA and dsDNA (ssDNA + ssDNA′) targets are presented below.

ssDNA (5′-3′; binding sequence underlined):
GGTGCAAAGAGGCATGATACATTGTATCATTAT<u>TGCCCTGAAAGAAAGAGA</u>TTAGG GAAAGTATTAGAAATAAGATAAAC.

ssDNA′ (5′-3′):
GTTTATCTTATTTCTAATACTTTCCCTAATCTCTTTCTTTCAGGGCAATAATGATACA ATGTATCATGCCTCTTTGCACC.

Thermal denaturation analyses

Melting curves were generated by recording UV absorbance at 265 nm with increasing temperature on a Chirascan CD spectropolarimeter equipped with a thermoelectrically regulated multicell holder. All samples were prepared by annealing solutions containing 2.5 μM ssDNA/dsDNA and 5 μM PNA/γPNA in 10 or 100 mM NaPi buffer (pH 7.4). Absorbance measurements were recorded after every 1°C change while applying a temperature ramp rate of 1°C/min. Where possible, van't Hoff analyses of the melting curves were performed using the protocols developed by Marky and Breslauer.[51] Briefly, the UV melting curves were transformed into α plots to denote the fraction of single strands in hybridized form at each measured temperature. The temperature at α = 0.5 is the melting temperature (Tm) of the hybrid (Table 2).

Electrophoretic mobility shift (gel-shift) assays and determination of dissociation constants

Strand invasion by each PNA/γPNA was evaluated using two different duplex substrates. First, 50 nM of a 100-mer dsDNA target, preassembled by hybridizing ssDNA with its complement (ssDNA[0]), was annealed with increasing equivalents (0- to 10-fold) of PNA/γPNA to assemble the most stable hybrid. Each sample was then run on a nondenaturing 8% polyacrylamide gel electrophoresis (PAGE) system (acrylamide:bis-acrylamide [19:1] [40%] [5 mL], Tris-borate-EDTA [TBE] buffer [5×] [5 mL], H_2O [14.625 mL], ammonium persulfate [10%] [250 μL], TEMED [25 μL]) in 1× TBE buffer (pH 7.4) at 120 V for 40 min. The gel was stained with 1× SYBR Gold (Invitrogen/Thermo Fisher Scientific, catalog #S11494) for 5 min and washed with 1× TBE for 20 min. Resolved bands for free and bound DNA were visualized on a BioRad Universal Hood II gel doc system, and the images were processed and inverted using Image Lab software (v.5.2.1, BioRad, Hercules, CA, USA). The concentration of the PNA-DNA complex after each addition of the PNA/γPNA oligomer was fit to a Langmuir isotherm (Equation 1) that accounts for ligand depletion in GraphPad Prism v.8.0.1, as outlined in Oyaghire et al.[50] and Yang et al.,[54] where $[P_T]$ is the total PNA/γPNA concentration, $[D_T]$ is the total dsDNA concentration, and K_D is the equilibrium dissociation constant.

$$[PNA - DNA] = \frac{[P_T] + [D_T] + [K_D] - \sqrt{([P_T] + [D_T] + [K_D])^2 - 4 \cdot [P_T] \cdot [D_T]}}{2}$$

NP formulation

PLGA NPs encapsulating PNA and donor DNA were formulated using a double-emulsion solvent evaporation technique. Briefly, 40 mg PLGA was dissolved in 1 mL dichloromethane (40 mg mL^{-1}). 40 μL donor DNA (1 mM) and 80 μL PNA (1 mM) were quickly mixed and added to the polymer solution dropwise while vortexing the polymer. The mixture was subsequently sonicated at 38% amplitude 3 times for 10 s using a probe sonicator. To form the second emulsion, the primary emulsion was added dropwise to 2 mL of a 5% (w/v) solution of PVA. The second emulsion was subsequently sonicated at 38% amplitude 3 times for 10 s using a probe sonicator. This mixture was finally poured into 20 mL 0.3% (w/v) PVA solution and stirred for 3 h at room temperature (360 rpm) while the NPs "hardened." NPs were subsequently pelleted by centrifugation at 16,100g for 15 min. The NP pellet was resuspended in 20 mL diH$_2$O and washed an additional 2 times, for a total of 3 centrifugation steps. The final NP pellet was resuspended in diH$_2$O with trehalose (5 mg/mL), such that the final ratio of NP:trehalose was 1 mg NP:1 mg trehalose. The final NP solution was flash frozen in liquid nitrogen, lyophilized for 48 h, and stored at −20°C until further use.

NP characterization

NP size and zeta potential were measured using the Malvern ZetaSizer as per manufacturer guidelines. Measurements were made in diH$_2$O at an NP concentration of 0.05 mg/mL. Total nucleic acid loading was determined by absorbance at 260 nm following de-formulation in DMSO. Total nucleic acid release was determined by incubating 2 mg NPs in 1 mL 1× PBS in a 37°C shaker. At specified time points, NPs were centrifuged at 21,000g; 950 μL of the supernatant was collected and replaced, followed by absorbance measurement at 260 nm. NPs were imaged by TEM. Briefly, TEM samples were negatively stained with 2% uranyl acetate. The imaging was performed at an acceleration voltage of 120 kV using a FEI Tecnai T12 TEM at the Center for Cellular and Molecular Imaging, Yale School of Medicine.

Ex vivo gene editing in primary bone marrow cells

Bone marrow cells were harvested by flushing the femurs and tibias of Townes mice containing the human β-globin transgene. 500,000 cells were subsequently treated with 2 mg mL^{-1} PLGA NPs in Roswell Park Memorial Institute (RPMI) medium supplemented with 20% FBS and 5% penn-strep. 72 h later, genomic DNA (gDNA) was harvested using the Promega ReliaPrep gDNA Tissue Miniprep System (Promega, Madison, WI, USA). Similarly, bone marrow cells from a mouse model of β-thalassemia with the IVS2-654 mutation[55] were flushed and treated with PLGA NPs containing PNA and a "correcting donor" DNA. As before, gDNA was harvested 72 h after NP treatment. DNA size selection was performed using the Ampure beads (1.8×) following gDNA extraction when comparing $^{ser}\gamma$PNA with $^{ser}\gamma$PNA-scr. In all cases, editing frequencies were quantified using a ddPCR method, which we previously developed and validated.[8]

Each ddPCR reaction consisted of up to 80 ng gDNA; 12.5 μL 2× ddPCR supermix for probes (no dUTP) (BioRad); 0.225 μL forward primer (100 μM); 0.225 μL reverse primer (100 μM); 0.063 mL β-thalassemia (β-thal) probe (100 μM); 0.063 μL wild-type probe (100 μM) (Integrated DNA Technologies, Coralville, IA, USA); 0.5 μL EcoR1; 11.424 μL gDNA; and dH_2O. Droplets were generated using the Automated Droplet Generator (AutoDG, BioRad). Thermocycling conditions were as follows: 95°C 10 min (94°C 30 s, 55.3°C 5 min – ramp 2°C/s) × 39 cycles, 98°C 10 min, hold at 4°C. Droplets were allowed to rest at 4°C for at least 30 min after cycling and were then read using the QX200 Droplet Reader (BioRad). Data were analyzed using QuantaSoft software. Data are represented as the fractional abundance of the wild-type allele. The primers used for ddPCR were as follows: forward (5′-3′): ACCATTCTAAAGAATAACAGTGA, reverse (5′-3′): CCTCTTACATCAGTTACAATTT. The probes used for ddPCR were as follows: wild type (5′-FAM): TGGGTTAAGGCAATAGCAA; β-thal (5′-HEX): TCTGGGTTAAGGTAATAGCAAT, where the base in bold is complementary to the targeted mutation site.

Supplementary Material

Refer to Web version on PubMed Central for supplementary material.

ACKNOWLEDGMENTS

REFERENCES

1. Rogers FA, Vasquez KM, Egholm M, and Glazer PM (2002). Site-directed recombination via bifunctional PNA–DNA conjugates. Proc. Natl. Acad. Sci. USA 99, 16695–16700. 10.1073/pnas.262556899. [PubMed: 12461167]

2. McNeer NA, Schleifman EB, Cuthbert A, Brehm M, Jackson A, Cheng C, Anandalingam K, Kumar P, Shultz LD, Greiner DL, et al. (2013). Systemic delivery of triplex-forming PNA and donor DNA by nanoparticles mediates site-specific genome editing of human hematopoietic cells in vivo. Gene Ther. 20, 658–669. 10.1038/gt.2012.82. [PubMed: 23076379]

3. Schleifman EB, McNeer NA, Jackson A, Yamtich J, Brehm MA, Shultz LD, Greiner DL, Kumar P, Saltzman WM, and Glazer PM (2013). Site-specific Genome Editing in PBMCs With PLGA Nanoparticle-delivered PNAs Confers HIV-1 Resistance in Humanized Mice. Mol. Ther. Nucleic Acids 2, e135. 10.1038/mtna.2013.59. [PubMed: 24253260]

4. Fields RJ, Quijano E, McNeer NA, Caputo C, Bahal R, Anandalingam K, Egan ME, Glazer PM, and Saltzman WM (2015). Modified Poly(lactic-co-glycolic Acid) Nanoparticles for Enhanced Cellular Uptake and Gene Editing in the Lung. Adv. Healthcare Mater 4, 361–366. 10.1002/adhm.201400355.

5. Schleifman EB, Bindra R, Leif J, del Campo J, Rogers FA, Uchil P, Kutsch O, Shultz LD, Kumar P, Greiner DL, and Glazer PM (2011). Targeted Disruption of the CCR5 Gene in Human Hematopoietic Stem Cells Stimulated by Peptide Nucleic Acids. Chem. Biol 18, 1189–1198. 10.1016/j.chembiol.2011.07.010. [PubMed: 21944757]

6. McNeer NA, Anandalingam K, Fields RJ, Caputo C, Kopic S, Gupta A, Quijano E, Polikoff L, Kong Y, Bahal R, et al. (2015). Nanoparticles that deliver triplex-forming peptide nucleic acid molecules correct F508del CFTR in airway epithelium. Nat. Commun 6, 6952. 10.1038/ncomms7952. [PubMed: 25914116]

7. Bahal R, Ali McNeer N, Quijano E, Liu Y, Sulkowski P, Turchick A, Lu Y-C, Bhunia DC, Manna A, Greiner DL, et al. (2016). In vivo correction of anaemia in β-thalassemic mice by γPNA-mediated gene editing with nanoparticle delivery. Nat. Commun 7, 13304. 10.1038/ncomms13304. [PubMed: 27782131]

8. Ricciardi AS, Bahal R, Farrelly JS, Quijano E, Bianchi AH, Luks VL, Putman R, López-Giráldez F, Co kun S, Song E, et al. (2018). In utero nanoparticle delivery for site-specific genome editing. Nat. Commun 9, 2481. 10.1038/s41467-018-04894-2. [PubMed: 29946143]

9. Baker M. (2012). Gene-editing nucleases. Nat. Methods 9, 23–26. 10.1038/nmeth.1807. [PubMed: 22312637]

10. Hsu PD, Lander ES, and Zhang F (2014). Development and Applications of CRISPR-Cas9 for Genome Engineering. Cell 157, 1262–1278. 10.1016/j.cell.2014.05.010. [PubMed: 24906146]

11. Paschon DE, Lussier S, Wangzor T, Xia DF, Li PW, Hinkley SJ, Scarlott NA, Lam SC, Waite AJ, Truong LN, et al. (2019). Diversifying the structure of zinc finger nucleases for high-precision genome editing. Nat. Commun 10, 1133. 10.1038/s41467-019-08867-x. [PubMed: 30850604]

12. Cullot G, Boutin J, Toutain J, Prat F, Pennamen P, Rooryck C, Teichmann M, Rousseau E, Lamrissi-Garcia I, Guyonnet-Duperat V, et al. (2019). CRISPR-Cas9 genome editing induces megabase-scale chromosomal truncations. Nat. Commun 10, 1136. 10.1038/s41467-019-09006-2. [PubMed: 30850590]

13. Kosicki M, Tomberg K, and Bradley A (2018). Repair of double-strand breaks induced by CRISPR–Cas9 leads to large deletions and complex rearrangements. Nat. Biotechnol 36, 765–771. 10.1038/nbt.4192. [PubMed: 30010673]

14. Haapaniemi E, Botla S, Persson J, Schmierer B, and Taipale J (2018). CRISPR–Cas9 genome editing induces a p53-mediated DNA damage response. Nat. Med 24, 927–930. 10.1038/s41591-018-0049-z. [PubMed: 29892067]

15. Lin Y, Cradick TJ, Brown MT, Deshmukh H, Ranjan P, Sarode N, Wile BM, Vertino PM, Stewart FJ, and Bao G (2014). CRISPR/Cas9 systems have off-target activity with insertions or deletions between target DNA and guide RNA sequences. Nucleic Acids Res. 42, 7473–7485. 10.1093/nar/gku402. [PubMed: 24838573]

16. Fu Y, Foden JA, Khayter C, Maeder ML, Reyon D, Joung JK, and Sander JD (2013). High-frequency off-target mutagenesis induced by CRISPR-Cas nucleases in human cells. Nat. Biotechnol 31, 822–826. 10.1038/nbt.2623. [PubMed: 23792628]

17. Simhadri VL, McGill J, McMahon S, Wang J, Jiang H, and Sauna ZE (2018). Prevalence of Pre-existing Antibodies to CRISPR-Associated Nuclease Cas9 in the USA Population. Mol. Ther. Methods Clin. Dev 10, 105–112. 10.1016/j.omtm.2018.06.006. [PubMed: 30073181]

18. Chew WL (2018). Immunity to CRISPR Cas9 and Cas12a therapeutics. WIREs Mechanisms. of. Disease 10, e1408. 10.1002/wsbm.1408.

19. Egholm M, Buchardt O, Christensen L, Behrens C, Freier SM, Driver DA, Berg RH, Kim SK, Norden B, and Nielsen PE (1993). PNA hybridizes to complementary oligonucleotides obeying the Watson–Crick hydrogen-bonding rules. Nature 365, 566–568. 10.1038/365566a0. [PubMed: 7692304]

20. Egholm M, Buchardt O, Nielsen PE, and Berg RH (1992). Peptide nucleic acids (PNA). Oligonucleotide analogs with an achiral peptide backbone. J. Am. Chem. Soc 114, 1895–1897. 10.1021/ja00031a062.

21. Kuhn H, Demidov VV, Nielsen PE, and Frank-Kamenetskii MD (1999). An experimental study of mechanism and specificity of peptide nucleic acid (PNA) binding to duplex DNA11 Edited by I. Tinoco. J. Mol. Biol 286, 1337–1345. 10.1006/jmbi.1998.2578.

22. Rogers FA, Lin SS, Hegan DC, Krause DS, and Glazer PM (2012). Targeted Gene Modification of Hematopoietic Progenitor Cells in Mice Following Systemic Administration of a PNA-peptide Conjugate. Mol. Ther 20, 109–118. 10.1038/mt.2011.163. [PubMed: 21829173]

23. Kim K-H, Nielsen PE, and Glazer PM (2007). Site-directed gene mutation at mixed sequence targets by psoralen-conjugated pseudo-complementary peptide nucleic acids. Nucleic Acids Res. 35, 7604–7613. 10.1093/nar/gkm666. [PubMed: 17977869]

24. Kim K-H, Nielsen PE, and Glazer PM (2006). Site-Specific Gene Modification by PNAs Conjugated to Psoralen. Biochemistry 45, 314–323. 10.1021/bi051379a. [PubMed: 16388608]

25. McNeer NA, Chin JY, Schleifman EB, Fields RJ, Glazer PM, and Saltzman WM (2011). Nanoparticles Deliver Triplex-forming PNAs for Site-specific Genomic Recombination in CD34+ Human Hematopoietic Progenitors. Mol. Ther 19, 172–180. 10.1038/mt.2010.200. [PubMed: 20859257]

26. Vermaak D, Ahmad K, and Henikoff S (2003). Maintenance of chromatin states: an open-and-shut case. Curr. Opin. Cell Biol 15, 266–274. 10.1016/S0955-0674(03)00043-7. [PubMed: 12787767]

27. Egholm M, Christensen L, Dueholm KL, Buchardt O, Coull J, and Nielsen PE (1995). Efficient pH-independent sequence-specific DNA binding by pseudoisocytosine-containing bis-PNA. Nucleic Acids Res. 23, 217–222. 10.1093/nar/23.2.217. [PubMed: 7862524]

28. Bentin T, Larsen HJ, and Nielsen PE (2003). Combined Triplex/Duplex Invasion of Double-Stranded DNA by "Tail-Clamp" Peptide Nucleic Acid. Biochemistry 42, 13987–13995. 10.1021/bi0351918. [PubMed: 14636067]

29. Sahu B, Sacui I, Rapireddy S, Zanotti KJ, Bahal R, Armitage BA, and Ly DH (2011). Synthesis and Characterization of Conformationally Preorganized, (R)-Diethylene Glycol-Containing γ-Peptide Nucleic Acids with Superior Hybridization Properties and Water Solubility. J. Org. Chem 76, 5614–5627. 10.1021/jo200482d. [PubMed: 21619025]

30. Dragulescu-Andrasi A, Rapireddy S, Frezza BM, Gayathri C, Gil RR, and Ly DH (2006). A Simple γ-Backbone Modification Preorganizes Peptide Nucleic Acid into a Helical Structure. J. Am. Chem. Soc 128, 10258–10267. 10.1021/ja0625576. [PubMed: 16881656]

31. Bahal R, Sahu B, Rapireddy S, Lee C-M, and Ly DH (2012). Sequence-Unrestricted, Watson–Crick Recognition of Double Helical B-DNA by (R)-MiniPEG-γPNAs. Chembiochem 13, 56–60. 10.1002/cbic.201100646. [PubMed: 22135012]

32. Yeh JI, Shivachev B, Rapireddy S, Crawford MJ, Gil RR, Du S, Madrid M, and Ly DH (2010). Crystal Structure of Chiral γPNA with Complementary DNA Strand: Insights into the Stability and Specificity of Recognition and Conformational Preorganization. J. Am. Chem. Soc 132, 10717–10727. 10.1021/ja907225d. [PubMed: 20681704]

33. Eriksson M, and Nielsen PE (1996). Solution structure of a peptide nucleic acid–DNA duplex. Nat. Struct. Biol 3, 410–413. 10.1038/nsb0596-410. [PubMed: 8612069]

34. Englund EA, and Appella DH (2005). Synthesis of γ-Substituted Peptide Nucleic Acids: A New Place to Attach Fluorophores without Affecting DNA Binding. Org. Lett 7, 3465–3467. 10.1021/ol051143z. [PubMed: 16048318]

35. Calabretta A, Tedeschi T, Corradini R, Marchelli R, and Sforza S (2011). DNA and RNA binding properties of an arginine-based 'Extended Chiral Box' Peptide Nucleic Acid. Tetrahedron Lett. 52, 300–304. 10.1016/j.tetlet.2010.11.034.

36. Kirillova Y, Boyarskaya N, Dezhenkov A, Tankevich M, Prokhorov I, Varizhuk A, Eremin S, Esipov D, Smirnov I, and Pozmogova G (2015). Polyanionic Carboxyethyl Peptide Nucleic Acids (ce-PNAs): Synthesis and DNA Binding. PLoS One 10, e0140468. 10.1371/journal.pone.0140468. [PubMed: 26469337]

37. kumar P, and Jain DR (2015). Cγ-Aminopropylene peptide nucleic acid (amp-PNA): chiral cationic PNAs with superior PNA:DNA/RNA duplex stability and cellular uptake. Tetrahedron 71, 3378–3384. 10.1016/j.tet.2015.03.093.

38. Dezhenkov AV, Tankevich MV, Nikolskaya ED, Smirnov IP, Pozmogova GE, Shvets VI, and Kirillova YG (2015). Synthesis of anionic peptide nucleic acid oligomers including γ-carboxyethyl thymine monomers. Mendeleev Commun. 25, 47–48. 10.1016/j.mencom.2015.01.017.

39. Tähtinen V, Granqvist L, Murtola M, Strömberg R, and Virta P (2017). 19F NMR Spectroscopic Analysis of the Binding Modes in Triple-Helical Peptide Nucleic Acid (PNA)/MicroRNA Complexes. Chemistry 23, 7113–7124. 10.1002/chem.201700601. [PubMed: 28370485]

40. Pensato S, Saviano M, Bianchi N, Borgatti M, Fabbri E, Gambari R, and Romanelli A (2010). γ-Hydroxymethyl PNAs: Synthesis, interaction with DNA and inhibition of protein/DNA interactions. Bioorg. Chem 38, 196–201. 10.1016/j.bioorg.2010.06.002. [PubMed: 20643471]

41. Mitra R, and Ganesh KN (2012). Aminomethylene Peptide Nucleic Acid (amPNA): Synthesis, Regio-/Stereospecific DNA Binding, And Differential Cell Uptake of (α/γ,R/S) am-PNA Analogues. J. Org. Chem 77, 5696–5704. 10.1021/jo300860f. [PubMed: 22676429]

42. Avitabile C, Moggio L, Malgieri G, Capasso D, Di Gaetano S, Saviano M, Pedone C, and Romanelli A (2012). γ sulphate PNA (PNA S): Highly Selective DNA Binding Molecule Showing Promising Antigene Activity. PLoS One 7, e35774. 10.1371/journal.pone.0035774. [PubMed: 22586450]

43. Sahu B, Chenna V, Lathrop KL, Thomas SM, Zon G, Livak KJ, and Ly DH (2009). Synthesis of Conformationally Preorganized and Cell-Permeable Guanidine-Based γ-Peptide Nucleic Acids (γGPNAs). J. Org. Chem 74, 1509–1516. 10.1021/jo802211n. [PubMed: 19161276]

44. Hsieh W-C, Shaikh AY, Perera JDR, Thadke SA, and Ly DH (2019). Synthesis of (R)- and (S)-Fmoc-Protected Diethylene Glycol Gamma PNA Monomers with High Optical Purity. J. Org. Chem 84, 1276–1287. 10.1021/acs.joc.8b02714. [PubMed: 30608165]

45. Manna A, Rapireddy S, Sureshkumar G, and Ly DH (2015). Synthesis of optically pure γPNA monomers: a comparative study. Tetrahedron 71, 3507–3514. 10.1016/j.tet.2015.03.052. [PubMed: 30792557]

46. Sacui I, Hsieh W-C, Manna A, Sahu B, and Ly DH (2015). Gamma Peptide Nucleic Acids: As Orthogonal Nucleic Acid Recognition Codes for Organizing Molecular Self-Assembly. J. Am. Chem. Soc 137, 8603–8610. 10.1021/jacs.5b04566. [PubMed: 26079820]

47. Nakanishi K, Berova N, and Woody RW (2000). Circular Dichroism : Principles and Applications (VCH).

48. Crawford MJ, Rapireddy S, Bahal R, Sacui I, and Ly DH (2011). Effect of Steric Constraint at the γ-Backbone Position on the Conformations and Hybridization Properties of PNAs. J. Nucleic Acids 2011, 652702. 10.4061/2011/652702. [PubMed: 21776375]

49. Datta B, and Armitage BA (2001). Hybridization of PNA to structured DNA targets: quadruplex invasion and the overhang effect. J. Am. Chem. Soc 123, 9612–9619. 10.1021/ja016204c. [PubMed: 11572682]

50. Oyaghire SN, Cherubim CJ, Telmer CA, Martinez JA, Bruchez MP, and Armitage BA (2016). RNA G-Quadruplex Invasion and Translation Inhibition by Antisense γ-Peptide Nucleic Acid Oligomers. Biochemistry 55, 1977–1988. 10.1021/acs.biochem.6b00055. [PubMed: 26959335]

51. Marky LA, and Breslauer KJ (1987). Calculating thermodynamic data for transitions of any molecularity from equilibrium melting curves. Biopolymers 26, 1601–1620. 10.1002/bip.360260911. [PubMed: 3663875]

52. Rapireddy S, He G, Roy S, Armitage BA, and Ly DH (2007). Strand Invasion of Mixed-Sequence B-DNA by Acridine-Linked, γ-Peptide Nucleic Acid (γ-PNA). J. Am. Chem. Soc 129, 15596–15600. 10.1021/ja074886j. [PubMed: 18027941]

53. Manna A, Rapireddy S, Bahal R, and Ly DH (2014). MiniPEG-γPNA. In Peptide Nucleic Acids: Methods and Protocols, Second Edition, Nielsen PE and Appella DH, eds. (Humana Press), pp. 1–12. 10.1007/978-1-62703-553-8_1.

54. Yang L, Toh DFK, Krishna MS, Zhong Z, Liu Y, Wang S, Gong Y, and Chen G (2020). Tertiary Base Triple Formation in the SRV-1 Frameshifting Pseudoknot Stabilizes Secondary Structure Components. Biochemistry 59, 4429–4438. 10.1021/acs.biochem.0c00611. [PubMed: 33166472]

55. Bahal R, Ali McNeer N, Quijano E, Liu Y, Sulkowski P, Turchick A, Lu YC, Bhunia DC, Manna A, Greiner DL, et al. (2016). In vivo correction of anaemia in beta-thalassemic mice by gammaPNA-mediated gene editing with nanoparticle delivery. Nat. Commun 7, 13304. 10.1038/ncomms13304. [PubMed: 27782131]

Highlights

Hydroxymethyl-γ modified PNAs are helically preorganized

The hydroxymethyl-γ modification affords more efficient DNA strand invasion

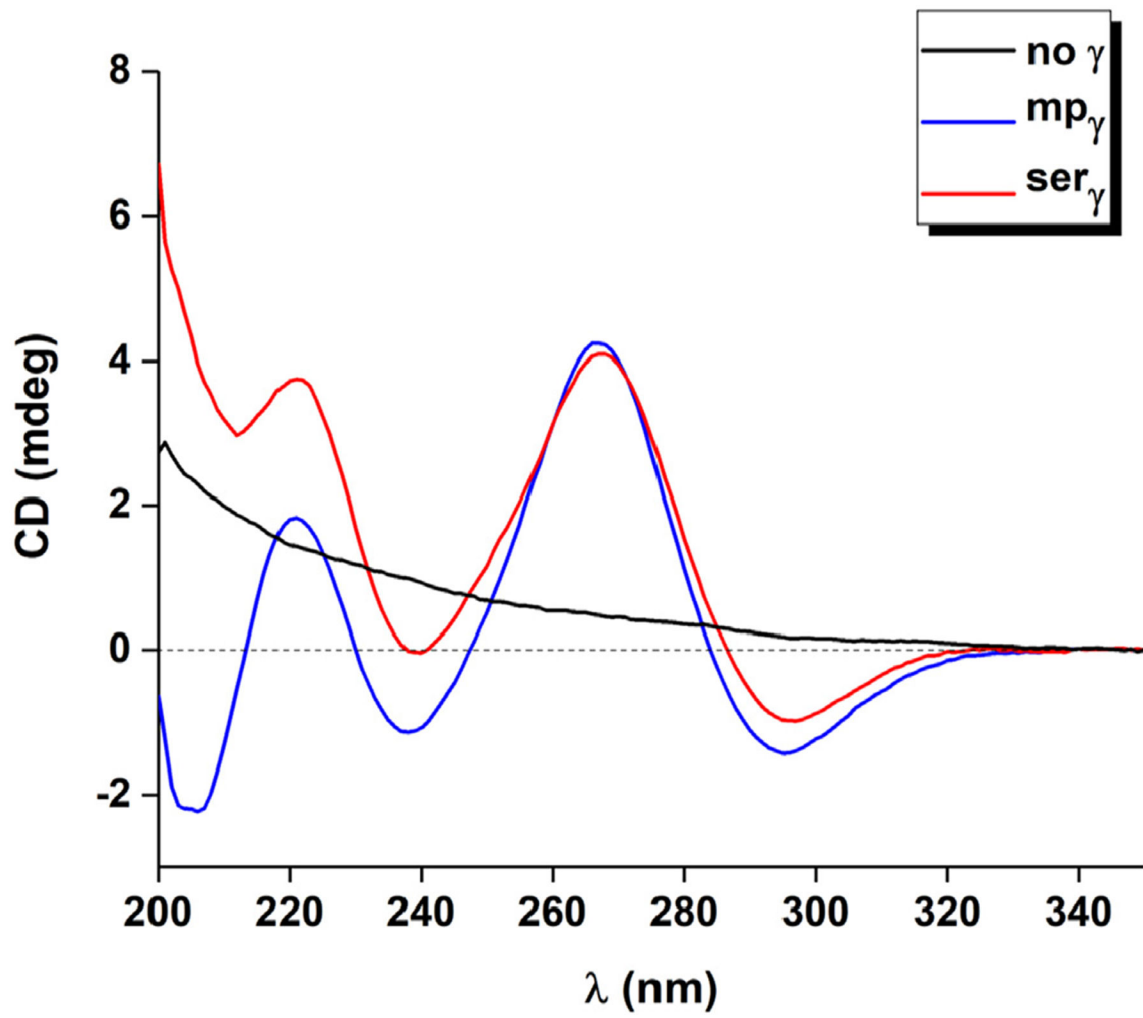PLGA nanoparticles containing these PNAs are superior at inducing gene modification

Figure 1. CD spectra for PNA, $^{mp}\gamma$PNA, and $^{ser}\gamma$PNA
All samples contained 20 μM of the respective oligomer in 10 mM NaPi buffer. Spectra were recorded at 37°C. Regular PNA (black), $^{mp}\gamma$PNA (blue), and $^{ser}\gamma$PNA (red).
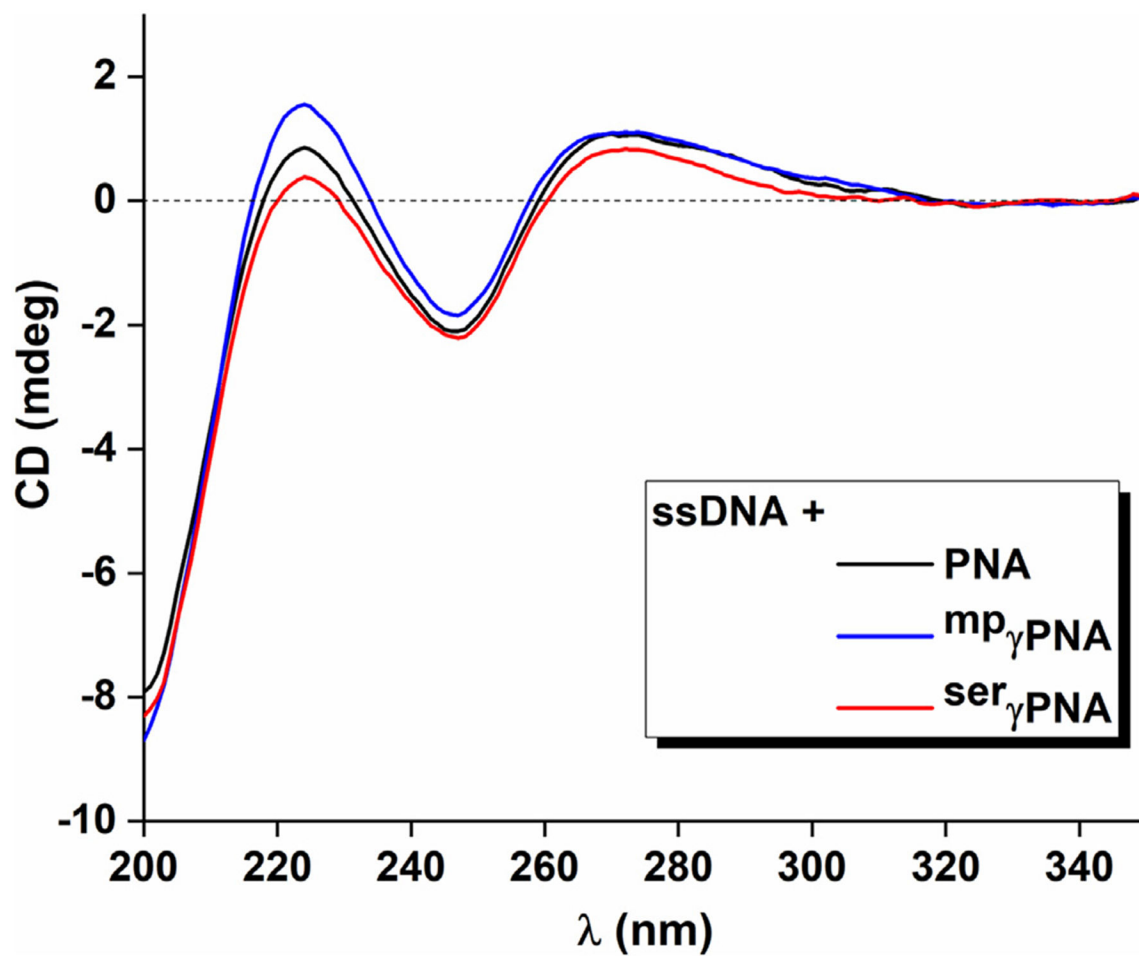
Figure 2. CD spectra for hybrid triplexes containing ssDNA and PNA, $^{mp}\gamma$PNA, or $^{ser}\gamma$PNA
All samples contained 1 μM ssDNA and 2 μM PNA/γPNA in 10 mM NaPi buffer. Spectra were recorded at 37°C. ssDNA and PNA (black), $^{mp}\gamma$PNA (blue), $^{ser}\gamma$PNA (red).
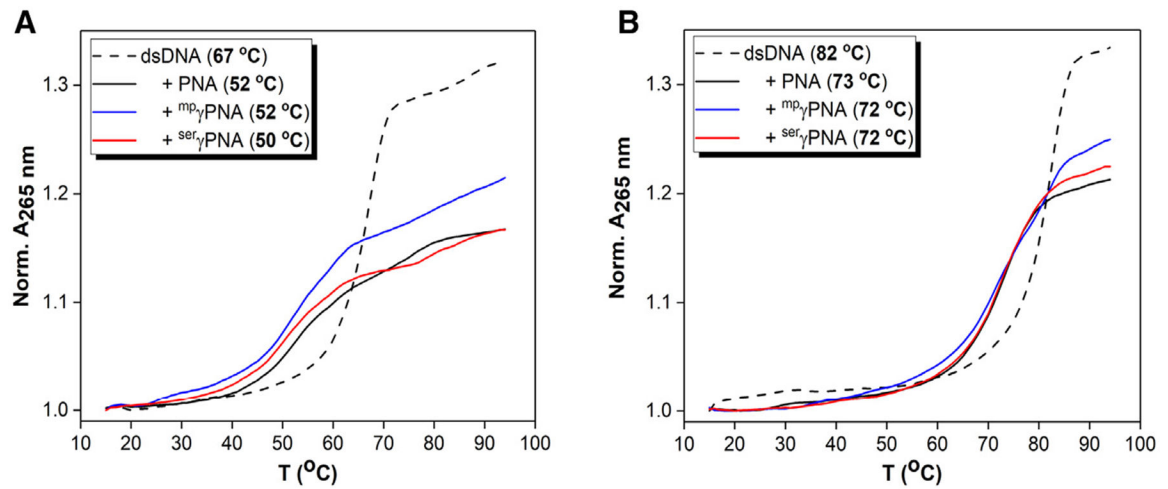
Figure 3. UV-thermal denaturation analyses on a 90-mer dsDNA alone or in combination with PNA, $^{mp}\gamma$PNA, or $^{ser}\gamma$PNA

All samples contained 2.5 μM dsDNA and 5 μM PNA/γPNA in 10 mM NaPi (A) or 100 mM NaPi (B). All samples were annealed as described in the experimental procedures, and melting temperature (Tm) values are presented in parentheses in the legend. 90-mer dsDNA alone (broken black) or in combination with PNA (solid black), $^{mp}\gamma$PNA (blue), and seryPNA (solid red).
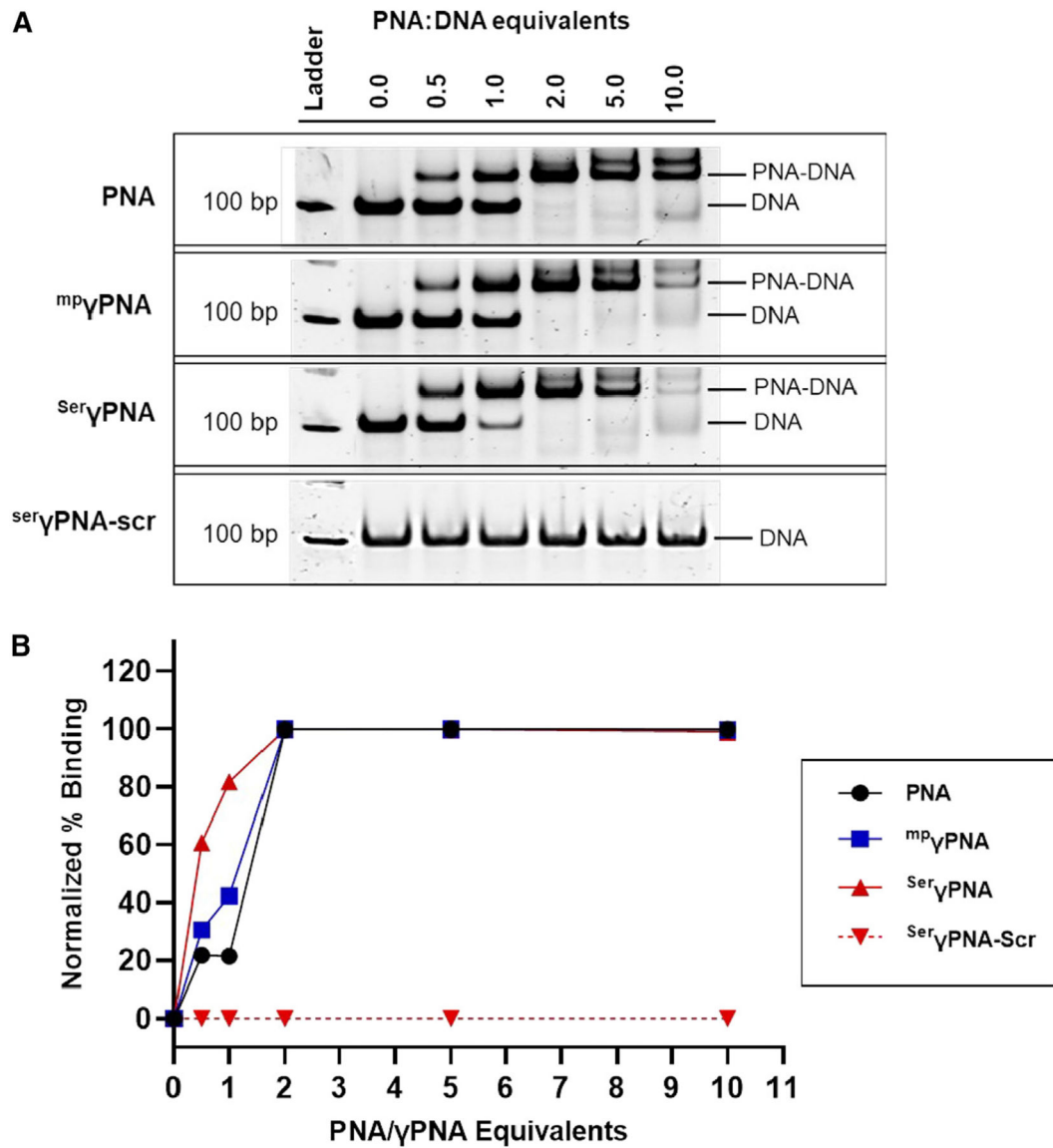
Figure 4. Titration of 100-mer dsDNA target with increasing equivalents of PNA, ^{mp}γPNA, ^{ser}γPNA, or ^{ser}γPNA-scr

(A) Each sample contained 50 nM DNA in 100 mM NaPi buffer, was annealed as in the experimental procedures, and was run on an 8% PAGE gel.

(B) The band intensities for the PNA-DNA hybrids were measured on ImageJ and normalized to the 0 equiv condition.
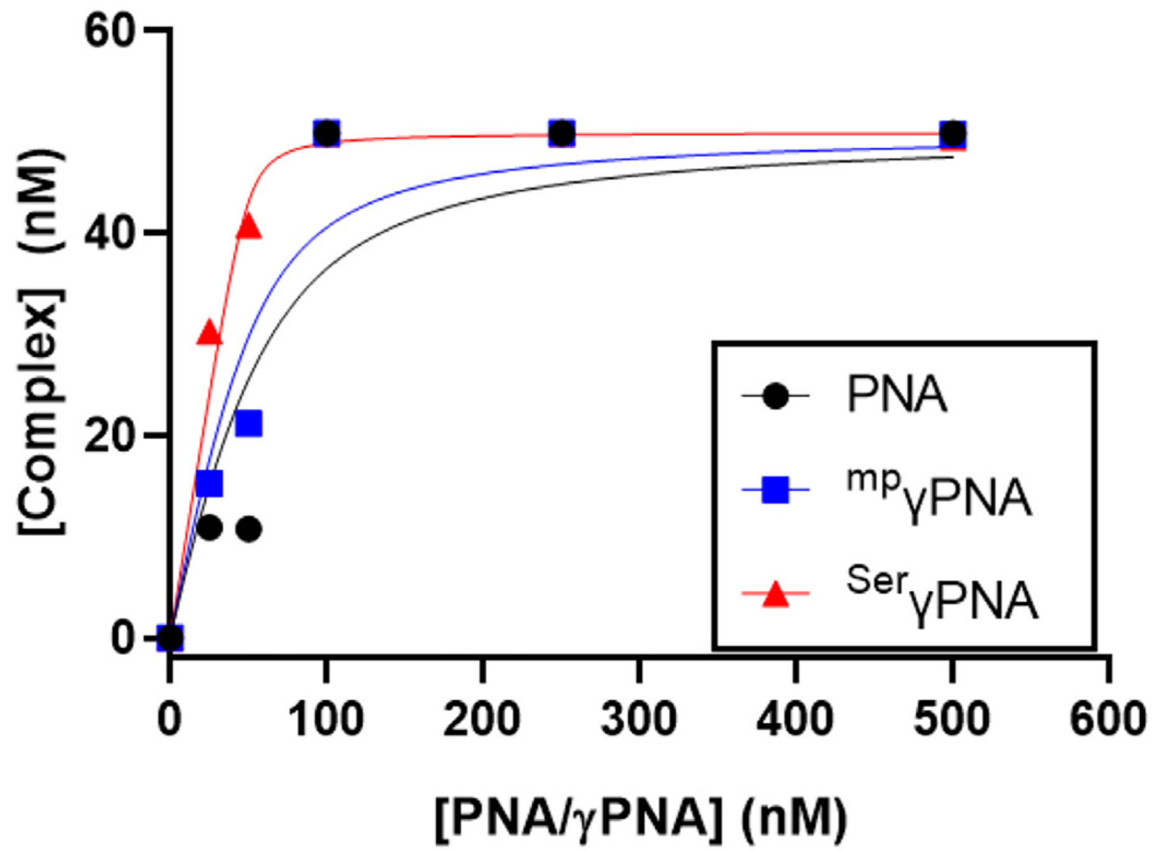
Figure 5.
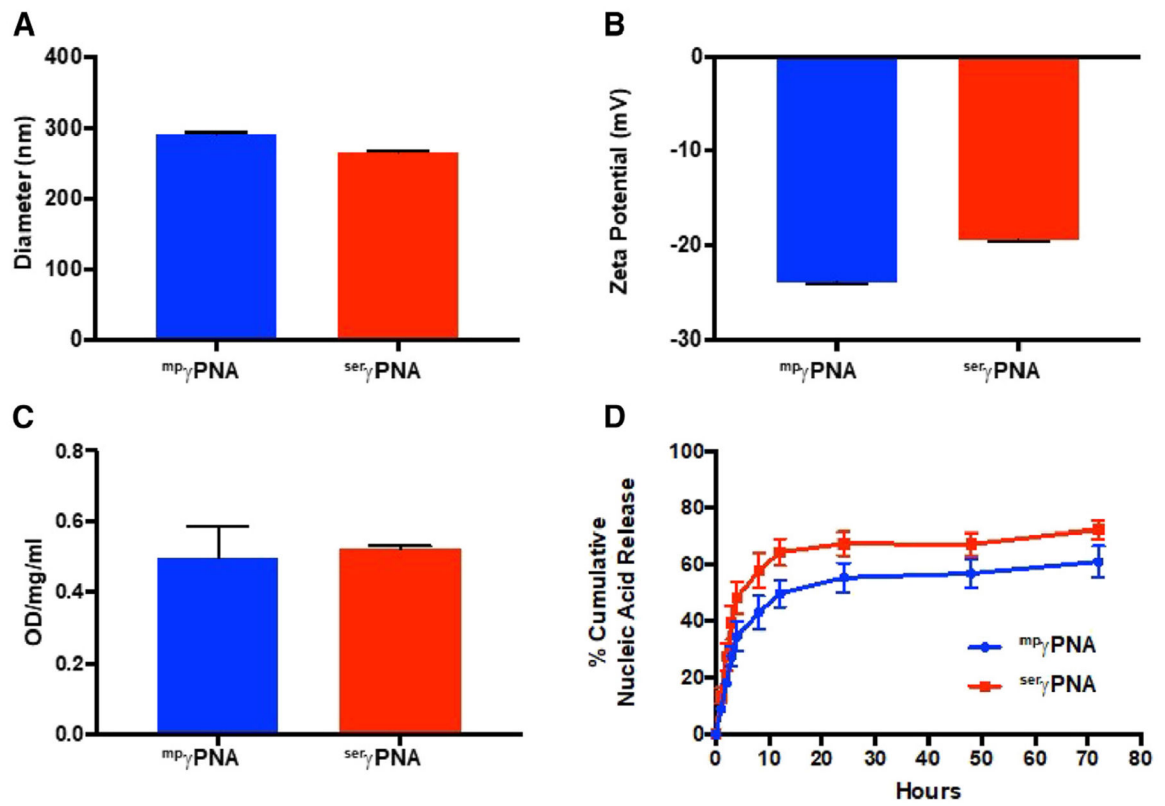Langmuir binding isotherms for PNA/γPNA complexes with dsDNA in 100 mM NaPi

Figure 6. NP characterization

(A) NP diameter as measured by dynamic light scattering (DLS).

(B) NP surface charge as measured by zeta potential.

(C) Total nucleic acid loading (PNA + donor DNA) in PLGA NPs.

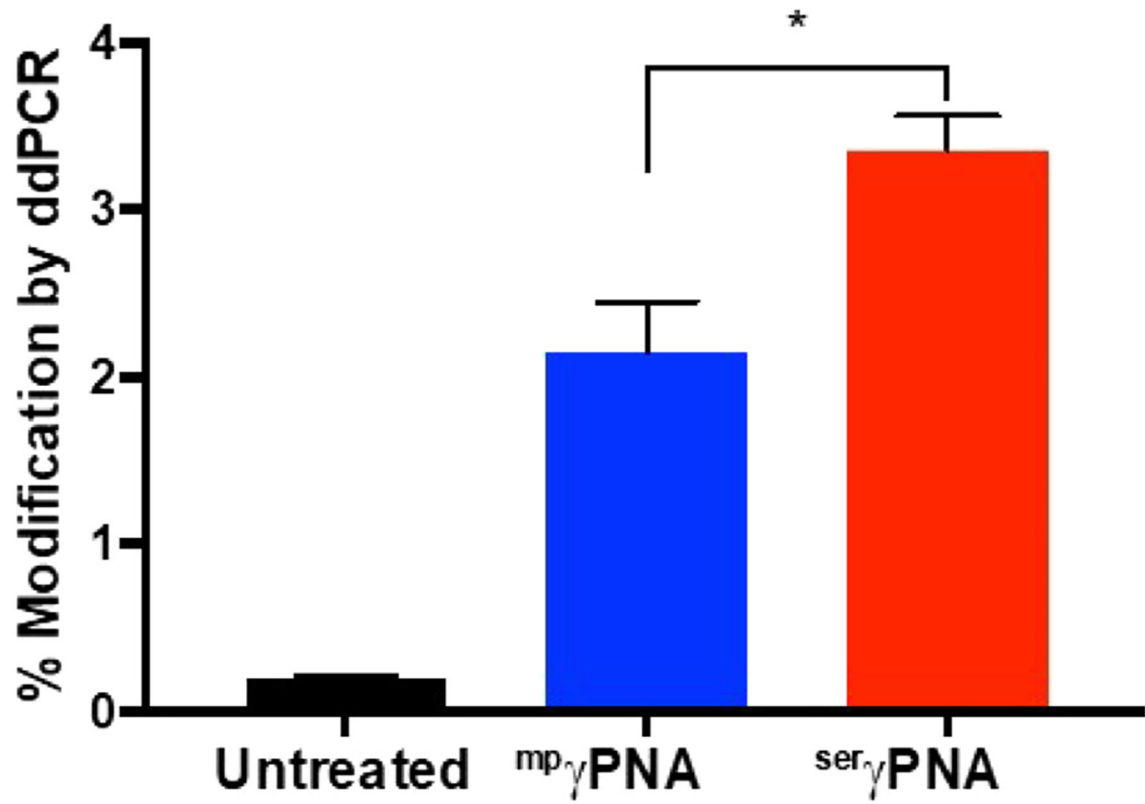(D) Release of nucleic acids from PLGA NPs. Error bars: mean with SD.

Figure 7. Modification of primary bone marrow cells with the β-thalassemia-causing mutation at IVS2-654

Bone marrow cells (BMCs) were left untreated (black) or were treated with NPs containing mpγPNA (blue) or serγPNA (red). Error bars: mean with SD. *p < 0.05.
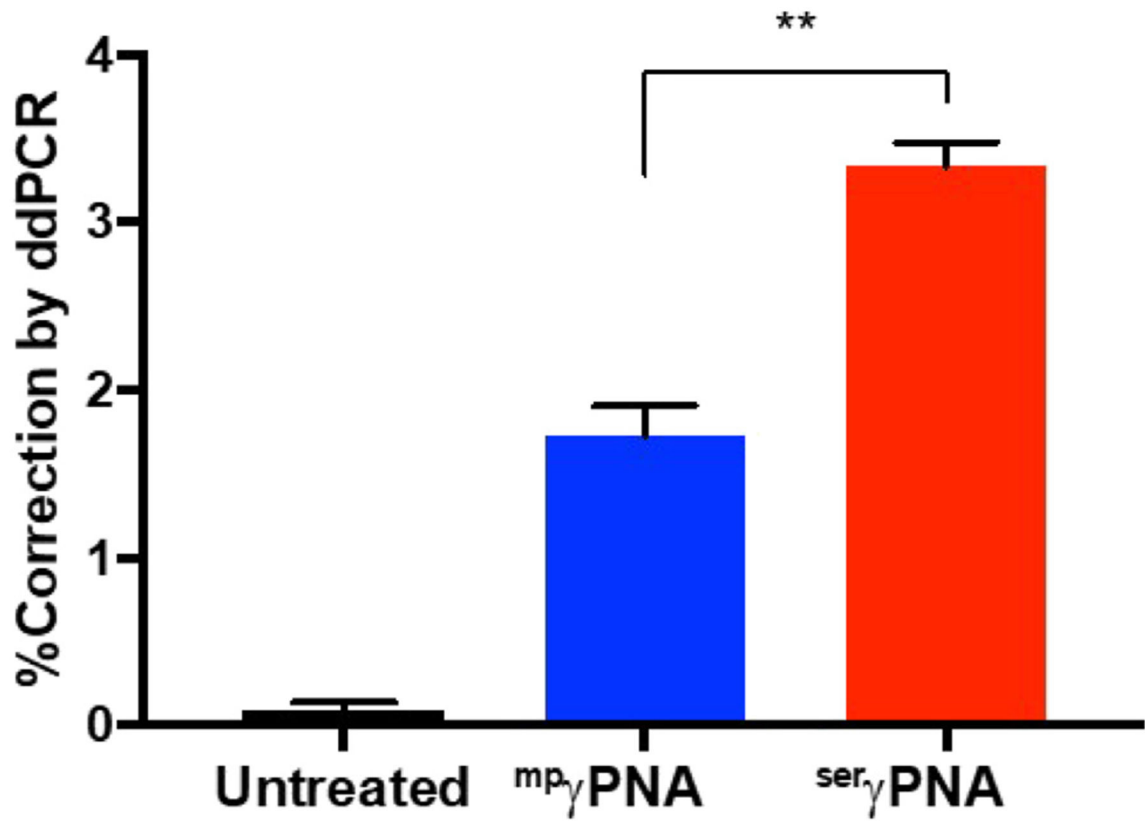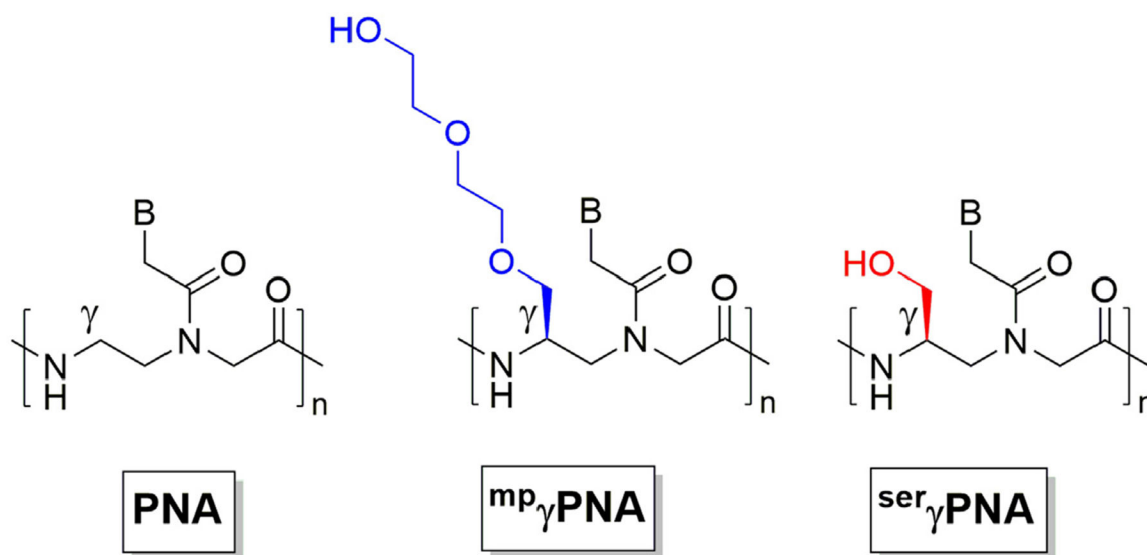
Figure 8. Correction of the β-thalassemia-causing mutation in primary BMCs

BMCs were left untreated (black) or were treated with NPs containing $^{mp}\gamma$PNA (blue) or $^{ser}\gamma$PNA (red). Error bars: mean with SD. **p < 0.005.

Scheme 1.
Chemical structures of PNA, $^{mp}\gamma$PNA, and $^{ser}\gamma$PNA monomer units

Table 1.

Sequences of $^{ser}\gamma$PNA, $^{ser}\gamma$PNA-scr, $^{mp}\gamma$PNA, and PNA oligomers

Oligomer	Sequence
$^{ser}\gamma$PNA	JTTTJTTTJTJT-OOO-TCTCTTTCTTTCAGGGCA
$^{ser}\gamma$PNA-scr	TJJTTTJTJTTT-OOO-CTTCGCAGACTTCTGTTT
$^{mp}\gamma$PNA (published as γtcPNA4[7])	JTTTJTTTJTJT-OOO-TCTCTTTCTTTCAGGGCA
PNA	JTTTJTTTJTJT-OOO-TCTCTTTCTTTCAGGGCA

All γPNA/PNAs are presented from N to C termini and have three consecutive lysine residues on each terminus. J, pseudoisocytidine,[27] a cytosine isomer that mimics the protonated form of cytosine and can thus form Hoogsteen H-bonds under neutral pH conditions; OOO, 11-amino-3,6,9-trioxaundecanoic acid linker between PNA domains designed to bind the Watson-Crick and Hoogsteen faces of the target DNA. Underlined sequences denote positions of γ modification.

Table 2.

Thermodynamic characterization of PNA/γPNA hybrids with dsDNA target

Hybrid	– G (kcal mol^{-1})	– H (kcal mol^{-1})	– S (cal mol^{-1} K^{-1})	Tm (°C)
10 mM NaPi[a]				
PNA/DNA	35 ± 3	77 ± 8	141 ± 20	52 ± 1
mpγPNA/DNA	34 ± 4	69 ± 5	118 ± 11	52 ± 1
serγPNA/DNA	34 ± 2	74 ± 8	134 ± 13	50 ± 1
100 mM NaPi[a]				
PNA/DNA	48 ± 3	139 ± 11	306 ± 16	73 ± 2
mpγPNA/DNA	41 ± 6	94 ± 8	176 ± 10	72 ± 1
serγPNA/DNA	45 ± 5	124 ± 9	264 ± 11	72 ± 1

[a]All values are calculated for 25°C.

Table 3.

Equilibrium dissociation constants for binding of PNA/γPNA oligomers to DNA duplex target

Oligomer	K_D (nM)
PNA	3.8
mpγPNA	2.2
serγPNA	0.2